Generation of short-chained granular corn starch by maltogenic α-amylase and transglucosidase treatment

Yuyue Zhong [a], Thewika Keeratiburana [b], Jacob Judas Kain Kirkensgaard [c], Bekzod Khakimov [c], Andreas Blennow [a],[*], Aleksander Riise Hansen [a],[*]

[a] Department of Plant and Environmental Sciences, University of Copenhagen, DK-1871 Frederiksberg C, Denmark
[b] Department of Food Science, Faculty of Science, Buriram Rajabhat University, Buriram, 31000, Thailand
[c] Department of Food Science, University of Copenhagen, DK-1958 Frederiksberg C, Denmark

ARTICLE INFO

ABSTRACT

We describe a method for permitting efficient modification by transglucosidase (TGA), from glycoside hydrolase family 31 (GH31), sequentially after the pre-treatment by maltogenic α-amylases (MA) from GH13. TGA treatment without MA pre-treatment had negligible effects on native starch, while TGA treatment with MA pre-treatment resulted in porous granules and increased permeability to enzymes. MA→TGA treatments lead to decreased molecular size of amylopectin molecules, increased α-1,6 branching, and increased amounts of amylopectin chains with the degree of polymerization (DP)<10 and decreased amounts of DP 10-28 after debranching. Wide-angle X-ray scattering (WAXS) data showed a general decrease in crystallinity except for a long term (20 h) TGA post-treatment which increased the relative crystallinity back to normal. MA→TGA treatment significantly lowered the starch retrogradation of starch and retarded the increase of storage- and loss moduli during storage. This work demonstrates the potential of sequential addition of starch active enzymes to obtain granular starch with improved functionality.

1. Introduction

Starch is synthesized and stored in the cell in the form of granules. So-called storage starch is deposited in amyloplasts and provide long term deposit of energy in grains, seeds, tubers and root organs. Maize (*Zea maize*), represents one of the world's most utilized domesticated crops for the production of food, feed, fuel and chemicals. The compact solid nature of the starch granule is mainly an effect of the efficient molecular packing of its two major components, amylose and amylopectin. As an effect, this compact structure does not readily permit access of proteins like enzymes to its inner part. Therefore, enzymatic modification of starch is typically carried out on gelatinized soluble starch at high temperatures. Maintaining the granule structure of starch is attractive for industry (Li et al., 2017), since it avoids handling issues associated with highly viscous systems and instability, e.g. retrogradation. Customization of native starch comes with its own challenges, but could ease supply chains from processing- to the application site.

When subjected to modification at sub-gelatinization temperatures the intrinsic structural features of the starch granules only permits a few classes of starch active enzymes to extensively modify the physichemical properties of starch (Blazek & Gilbert, 2010). One suggested mechanism to increase the efficiency of such processes has been to increase the accessible surface by producing pores on the surface of starch granules by hydrolases (Keeratiburana, Hansen, Soontaranon, Tongta, & Blennow, 2020) or by physical treatments alone (Szymońska & Wodnicka, 2005; Zhang, Han, & Lim, 2018) or in combination with hydrolases (Keeratiburana, Hansen, Soontaranon, Blennow, & Tongta, 2020; Keeratiburana, Hansen, Soontaranon, Tongta et al., 2020; Szymońska & Wodnicka, 2005), thereby increasing potential sites for enzyme catalysis. Dependent on the botanical origin, data from maize starch suggest that only *exo* active enzymes like amyloglucosidase and a few additional amylases were able to produce pores on the granular surface, while *endo* active cyclodextrin glycosyltransferase and branching enzymes had negligible effects (Benavent-Gil & Rosell, 2017).

Our recent data suggest that maltogenic α-amylase (MA) from GH13, commonly used in the bakery for anti-staling purpose, is capable of granular enzymatic modification at sub gelatinization temperatures (Keeratiburana, Hansen, Soontaranon, Blennow et al., 2020;

Table 1
The experiment design, yield, and amylose content of samples.

	Buffer only	MA	TGA	TGA time (h)	Yield (%)	Amylose content (%)
NMS	No	No	No	0	100.0 ± 0.0^a	30.7 ± 1.2^a
Buffer	Yes	No	No	0	95.0 ± 1.2^b	27.9 ± 0.4^a
TGA	Yes	No	9100 U/g	20	92.3 ± 2.1^b	28.6 ± 2.4^a
MA 3h	Yes	52 U/g	No	0	80.2 ± 0.4^c	29.0 ± 1.0^a
MATGA 6 h	Yes	52 U/g	9100 U/g	6	57.8 ± 0.8^d	28.0 ± 1.6^a
MATGA 20 h	Yes	52 U/g	9100 U/g	20	53.0 ± 1.1^e	29.0 ± 1.2^a

Keeratiburana, Hansen, Soontaranon, Tongta et al., 2020). Among the numerous characterized features of MA, it exhibits mainly *exo*-activity releasing successive maltose in the α-configuration. Unlike other *exo*-active enzymes like β-amylase (BA) and glucoamylase, MA also exhibits *endo*-glucanase activity. In addition to its structural similarity to cyclodextrinases (CGTases), MA is capable to both transglycosylate and hydrolyze maltotriose at high substrate concentration (Christophersen, Otzen, Noman, Christensen, & Schäfer, 1998). In this study, MA was used in combination with transglucosidase (TGA) from GH31. TGA is classified as an α-glucosidase (EC 3.2.1.20) that mainly acts as a glucose-releasing *exo* α-1-4 glucanase with high transglycosylation activity (Satoru Ishihara, 2017). TGA transfers glycosyl residues from longer maltooligosaccharides onto shorter α-glucans with DP2-8 creating new α-1-6 linkages via a double displacement mechanism (Ota, Okamoto, & Wakabayashi, 2009; Ota, Okamoto, Hoshino, & Wakabayashi, 2009). Hydrolysis of gelatinized starch and long soluble maltooligosaccharides derived from maize starch by maltogenic α-amylase and TGA, was reported to increase the relative proportion of α-1-6 linkages as detected by ^{1}H NMR (Ao et al., 2007). This effect was suggested to be due to the preferential hydrolysis of α-1-4 bonds and not the formation of new α-1-6 linkages by transglycosylation (Ota, Okamoto, & Wakabayashi, 2009; Ota, Okamoto, Hoshino et al., 2009). Methylation analysis of products obtained following incubation of gelatinized starch and maltooligosaccharides with TGA has suggested that the main reaction was α-1-4 hydrolysis since the product contained mainly shortened chains and not increased amounts of α-1-6 glycosidic linkages (Ota, Okamoto, & Wakabayashi, 2009; Ota, Okamoto, Hoshino et al., 2009). Sequential protocols using different α-amylases followed by β-amylase and/or TGA on granular starch have been reported for pea (Shi et al., 2014), cassava (Guo, Li et al., 2019) and sweet potato starch (Guo, Tao, Cui, & Janaswamy, 2019). The resulting granular starches showed increased contents of α-1-6 branched points and shorter amylopectin chains. Typically, the resulting starch had a narrower chain length distribution as deduced from gel permeation chromatography (GPC) after debranching, higher solubility, increased relative branching density, lower gelatinization temperatures and viscosities compared to control starches.

In this study, granular native maize starch was first modified by MA to generate porous starch, directly followed by TGA treatment. We hypothesized that using only MA, instead of complex combinations with *endo*-acting α-amylases and *exo*-acting β-amylases together with TGA, could be just as successful since we previously showed that amyloglucosidase and MA separately are capable to form porous rice starch granules (Keeratiburana, Hansen, Soontaranon, Blennow et al., 2020; Keeratiburana, Hansen, Soontaranon, Tongta et al., 2020).

2. Materials and methods

2.1. Starch and enzyme sources

Normal maize starch (NMS) (Commercial Clinton 106) was kindly provided by Archer Daniels Midland (ADM, Decatur, IL). The enzymes Maltogenic α-amylase (MA) (Maltogenase) at 41530 U/mL (Novozymes, Denmark) and Transglucosidase (TGA) from *Aspergillus niger* (TG-L2000) (Danisco, Singapore) at 22760 U/mL was kindly supplied. Debranching isoamylase and pullulanase were supplied from Megazyme (Ireland).

2.2. Successive modification on raw corn starch by maltogenic α-amylase and transglucosidase

The effects of the dosage and incubation time of MA and TGA on yield and viscosity were firstly explored by response surface methodology in triplicates. To optimize the yield of starch, the enzyme incubation time and concentration were selected (Table 1). Granules were first treated with MA (52 U/g) under stirring in 50 mM acetate buffer pH 5.5 with 5 mM CaCl2 at 10 % w/v at 50 °C for 3 h. The enzyme reaction was terminated on ice for 10 min, followed by the addition of 1 M NaOH to pH 11, and incubation for another 10 min. The pH was adjusted back to 5.5 by stepwise addition of 1 M HCl, and TGA (9100 U/g) was added for either 6 or 20 h at 50 °C. The reaction was terminated by repeating the pH adjustment from alkaline to neutral as above followed by 3 times water wash using centrifugation to remove the remaining salts. Starch samples were frozen overnight at -20 °C and freeze-dried. Three control samples were used: 1). NMS; 2). 20 h acetate buffer incubated NMS (abbreviation: Buffer); 3). 20 h TGA modified NMS (abbreviation: TGA).

2.3. Yield and amylose content

The yield was defined as the weight of non-soluble substrate relative to samples containing only the buffer. The amylose content was determined by triiodide colorimetry as described by Wickramasinghe, Blennow and Noda (2009).
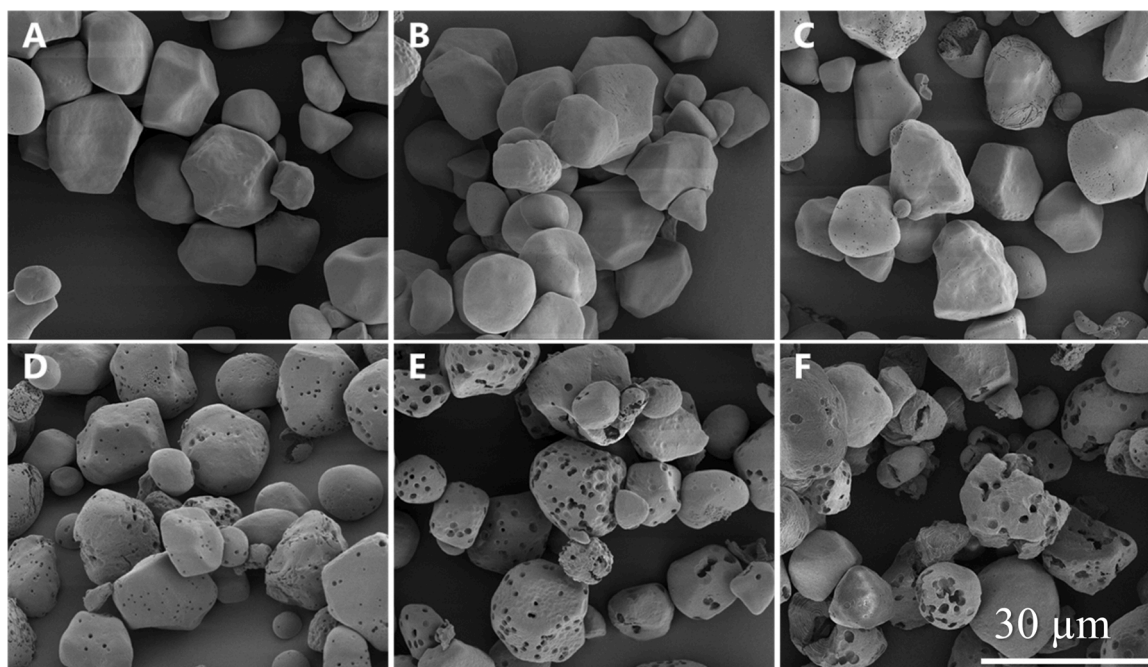
2.4. Scanning electron microscopy

Starch samples were fixed, sputter-coated with gold, and granular morphology was investigated using Field Emission Scanning Electron Microscopy (FE-SEM) (FEI Quanta 200).

2.5. Antibody labelling of granules and confocal laser scanning microscopy

Confocal Immunofluorescence Microscopy (CIM) was performed as follows. Starch granules were blocked with 5 % (w/v) skimmed milk powder in phosphate-buffered saline (M-PBS) for 30 min and then probed with the INCH1 anti-starch antibody (Rydahl, Hansen, Kračun, & Mravec, 2018) at 1:10 dilution, washed 3 times with PBS and probed with PBS secondary anti-mouse conjugated to AlexaFluor555 (Invitrogen) at 1:300 dilution. Both primary and secondary probing was done for 1 h. Skimmed milk powder is a common blocking agent when working with antibodies. It helps block unspecific binding and is used to adjust the signal/noise ratio. Antibody labelled granules were fixed in a 2 % agar 85 % glycerol matrix and mounted on a glass slide as described (Blennow et al., 2003). The scanning of fluorescently labelled sections was done on SP5 II confocal microscope (Leica) equipped with UV diode (405 nm), argon (488 nm) and helium-neon (543 nm) lasers.

2.6. High-performance anion exchange chromatography-pulsed amperometric detection (HPAEC-PAD)

Amylopectin molecular structure after debranching was analyzed as described (Song et al., 2019). In brief, 10 μL of gelatinized starch (5

Fig. 1. Scanning electron microscopy (SEM) of dried enzymatically treated granules. Native untreated maize corn granules (NMS) (A), incubation in buffer solution only (Buffer) (B) either treated alone with transglucosidase (TGA) (C) or maltogentic α-amylase alone (MA) (D) or followed by addition of transglucosidase for either 6 h (MATGA 6 h) (E) or 20 h (MATGA 20 h) (F).

mg/mL), debranched by isoamylase and pullulanase, was injected onto a CarboPac PA-200 column attached to an HPAEC-PAD (Dionex, Sunnyvale, CA, USA) system. Peak integration and detector response were performed as described (Blennow, Bay-Smidt, Wischmann, Olsen, & Møller, 1998).

2.7. Gel-permeation chromatography (GPC)

Native samples and debranched samples were analyzed using an SEC-TDA (Viscotek, Malvern, UK), equipped with tandem GS-520HQ / GS-320HQ Shodex columns attached to a TDA302 detector array, as described (Song et al., 2019). Briefly, 50 μL of samples (1 mg/mL) was injected and eluted in ammonium formate (10 mM), at a flow rate of 0.3 mL/min. The column temperatures were kept at 60 °C. Data analyses were performed using OmniSec Software 4.7 (Malvern Instrument, Ltd, UK). The pure maize amylose and amylopectin before and after debranching were used as standards.

2.8. Wide-angle X-ray scattering (WAXS)

Samples were conditioned at a humidity chamber with 90 % relative humidity for 48 h, and then analyzed using a SAXSLab instrument (JJ-X-ray, Copenhagen, Denmark) equipped with a 100 XL + microfocus sealed X-ray tube (Cu-K$_\alpha$ radiation, Rigaku, The Woodlands Texas, USA) and a 2D 300 K Pilatus detector (Dectris Ltd, Baden, Switzerland). Hydrated samples were sealed between 5−7 μm mica films to prevent any significant change in water content during the measurement, which was performed in a vacuum. The two-dimensional scattering data were azimuthally averaged and corrected for mica background using standard reduction software (SAXSGUI). The radially averaged intensity I is given as a function of the scattering angle 2θ in the angular range of 5°–30° using a wavelength of 0.1542 nm.

Relative crystallinity was calculated according to the methods described previously (Brückner, 2000; Goldstein et al., 2017). Amorphous background scattering was estimated using a 30-cycles iterative smoothing algorithm in MATLAB (Natick, Massachusetts, USA). The relative crystallinity was then estimated from the peak and total areas as

$$\text{Relative Crystallinity} = \text{Area of Peaks / Total Area} \tag{1}$$

where the areas are numerically integrated using built in MATLAB functions (Brückner, 2000; Goldstein et al., 2017).

2.9. Proton nuclear magnetic resonance (^{1}H NMR) spectroscopy

The degree of branching (DB) of starch was measured using one-dimensional ^{1}H NMR spectra acquired on 600 MHz NMR spectrometers (Bruker Avance III) from Bruker (Bruker Biospin, Rheinstetten, Germany). The spectrometer was equipped with an automated sample changer SampleJet (Bruker BioSpin), sample cooling and preheating station, a 5 mm broadband inverse RT (BBI) probe, and automated tuning and matching unit BCU-05. The starch samples (5%, w/w, starch to deuterium oxide) were gelatinized at 90 °C for 1 h in deuterium oxide and lyophilized. The freeze-dried samples were re-dissolved in deuterium oxide (containing 1.0 mg/mL 3-(Trimethylsilyl) propionic-2,2,3,3-d4 acid sodium salt (TSP)) at the concentration of 5% (w/w starch to D$_2$O) by heating at 90 °C for 0.5 h, and 0.6 mL solution was transferred into NMR glass tubes of 178 mm length and 5.0 mm diameter. Immediately after samples were analyzed by one-dimensional ^{1}H NMR spectroscopy at 60 °C. A 90° pulse experiment, with presaturation to suppress the residual water signal, was used to obtain ^{1}H NMR spectra with a recycle delay of 5 s. A total of 32 scans were obtained with a spectral width of 12,626 Hz resulting in 75k data points, and a total acquisition time of 2.99 s. Obtained free induction decay (FID) was apodized by Lorentzian line broadening of 0.3 Hz prior to Fourier Transformation. ^{1}H NMR spectra were then baseline and phase corrected using Topspin 4.0.7 (Bruker Biospin, Rheinstetten, Germany) and imported into SigMa software (https://doi.org/10.1016/j.aca.2020.02.025), where the area of signals representing anomeric protons (δ 5.35–5.45 α1,4; δ 4.95–5.00 α1,6; δ 5.20–5.24 α-anomeric reducing end protons; δ 4.64–4.68 β-anomeric reducing end protons) was calculated.
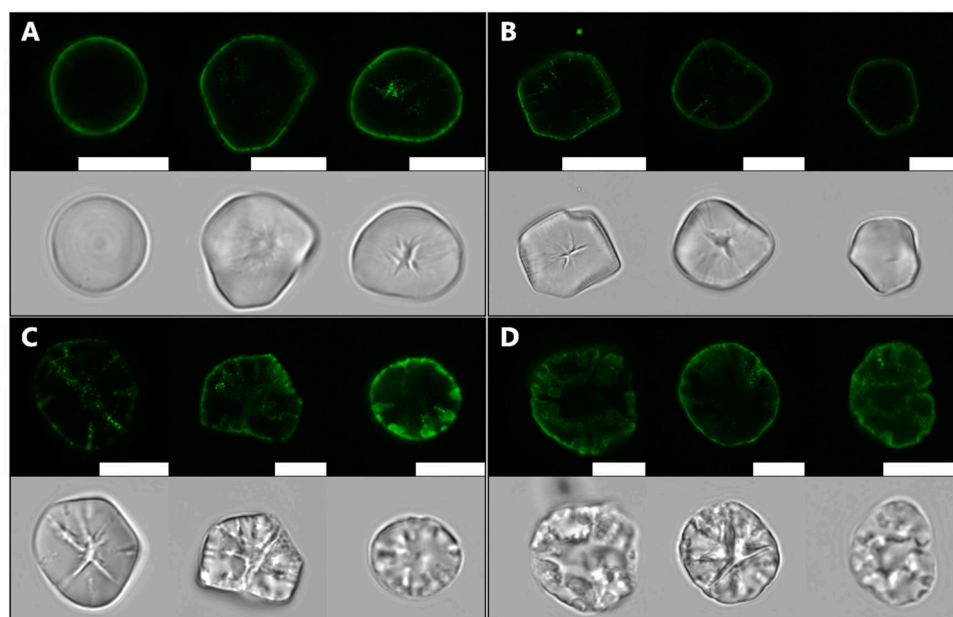
Fig. 2. Confocal Immunofluorescence Microscopy of 3 randomly selected maize granules after enzymatic treatment labelled with starch binding antibody INCH1 depicted trough fluorescent- and bright field channels. Native maize corn granules (NMS) (A) either treated alone with transglucosidase (TGA) alone (B) or maltogentic α-amylase (MA) alone (C) or both in sequential combination (MATGA 20 h) (D). Each granule is depicted individually with the vertical focus set from the center (scalebar = 10 μm).

2.10. Pasting- and dynamic gelling properties

The pasting properties were determined from 2.5 g starch suspended in 25 mL water (5 % w/v) by Rapid Visco Analyzer (RVA, Newport Scientific, Australia) using ICC Standard Method No. 162. The recorded pasting parameters were collected using Thermocline software for Windows (Perten Instruments, Sweden). The steady and dynamic rheological analysis was analyzed from 8 % (w/v) starch suspensions prepared from RVA, and measured using a Discovery HR-3 Rheometer (TA Instruments) at 25 °C. The gelatinized starches were measured directly and after storage for 7 days at 4 °C. Frequency sweeps were carried out from 0.01 to 100 Hz. The storage modulus, loss modulus, and complex viscosity were measured at 1 Hz in the linear viscoelastic region at 25 °C.

2.11. Water solubility and swelling power

Water solubility and swelling power were calculated as described by (Wang & Copeland, 2012). Briefly, 40 mg starch was suspended in 1 mL deionized water, mixed at 92.5 °C for 1 h, cooled down 20 °C, and centrifuged at 13,000*g* for 20 min. The supernatant was dried at 120 °C overnight and weighted and solubility was calculated based on the dried supernatant ratio to the original weight (40 mg).

2.12. Statistical analyses

Samples for WAXS and ^{1}H NMR analysis were performed once; all other experiments were performed in duplicate. Differences were analyzed using one-way analyses of variance (ANOVAs) followed by Duncan's test ($p < 0.05$) in SPSS 18.0 (SPSS Inc., Chicago, IL, USA).

3. Results

3.1. Maltogenic α-amylase pre-treatment permits modification with transglucosidase

To permit efficient enzyme modification by TGA, pre-treatment with MA was tested across different samples with varying concentrations and incubation time (data not shown). Both perforation and the overall yield of the samples decreased with an increased enzyme concentration and incubation time of both MA and TGA. Total this amounted to 16 samples with yields ranging 20–85 %. For applications, high yield is imperative, hence, only samples above 50 % yields were subjected to detailed analysis (Table 1). In order to keep track of the separate permutation to the reaction, each enzyme was individually added sequentially alongside a controlled starch only containing the buffered medium. Field Emission Scanning Electron Microscopy (FE-SEM, Fig. 1) revealed only very minor and narrow pore formation with TGA alone (Fig. 1C) but extensive pore formation and distribution on the surface of the granules catalyzed by MA (Fig. 1D). Based on the MA pre-treatment, TGA modified granules efficiently, confirmed by the larger pores on the surface of granules and partially disrupted granules (Fig. 1E and F). To further investigate whenever the pores extended deeper into the granules or only restricted to the surface, we studied the same samples using Confocal Immunofluorescence Microscopy (CIM) (Fig. 2). One way of visualizing if pores are permeable to enzymes is to use a fluorescent probe. Safranin and merbromine are traditionally stains for starch; however, their loosely defined specificity and small size contributed to their unspecified diffusion to various locations inside the granule (Naguleswaran, Li, Vasanthan, & Bressler, 2011). We speculated that the proteinaceous anti-starch antibody INCH1 (Rydahl et al., 2018), that recognizes linear α-1-4 glucan longer than 5 DP, would better simulate the permeability of enzymes. All samples were therefore labeled post-treatment with INCH1 for analysis by CIM. With the focus plane approximated to the middle of the granule the native corn- (Fig. 2A) and the TGA (Fig. 2B) starches revealed mostly INCH1 labelling on the outer surface with little to no irregularities on the surface. Minor very narrow pores could be indicated for the TGA only sample (Fig. 2B). However, when subject to MA treatment (Fig. 2C) more channels could be observed internally with the surface turned wrinkled and irregular both in fluoresces- and bright field channels. It is important to note that most maize granules contain internal cavities that can vary in depth and dimension with some extending through the hilum (Huber & BeMiller, 2000). The degree of degradation varied with some granules almost untouched, while others exhibited an almost destroyed hilum missing from the central cavity. When comparing yield, FE-SEM, and SIM data, we found TGA alone virtually failed to modify NMS granules while MA pre-treatment allowed efficient modification with TGA on granules. Therefore, we suggest effective TGA modification possibly requires the existence of internal channels which was produced by MA.
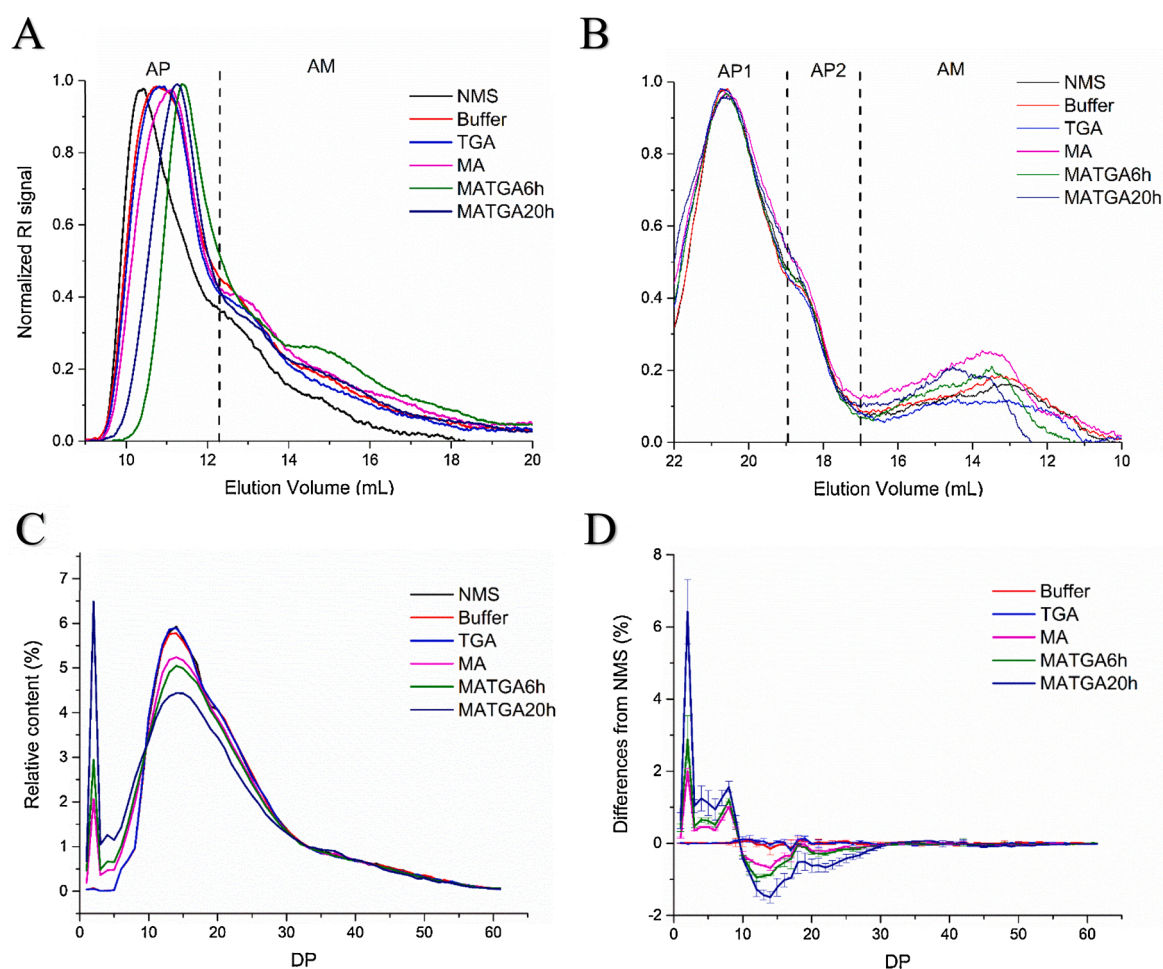
Fig. 3. Chain lengths distribution profiles of samples, a) raw starch characterized by GPC; b) debranched starch characterized by GPC; c) debranched amylopectin characterized by HPLEC-PAD; d) amylopectin chain length distribution difference plot from corresponding control NMS.

3.2. Chain length distribution (CLD)

CLD profiles as determined by Gel-permeation chromatography (GPC) of starch samples showed the 2 main molecules of starch: amylopectin (AP) and amylose (AM) fractions (Fig. 3A). The AP peak was shifted to a higher retention volume from NMS to Buffer, indicating the slight degradation of AP when NMS was incubated in the buffer. TGA alone samples showed a similar CLD profile compared with Buffer samples, reflecting a negligible change in the molecular structure of NMS by TGA. Degradation of AP was further aggravated after MA pre-treatment. It is worth mentioning 6 h TGA post-treatment resulted in further hydrolysis, while 20 h TGA post-treatment induced a minor shift of the AP fraction towards higher molecular size as compared to the 6 h TGA post-treatment. Such a shift indicates that the TGA exerts increased transglucosylation, that low molecular weight materials have been selectively removed and/or that there is the increased aggregation of the AP molecules. In the AM region, the area increased continuously from NMS to buffer, TGA, MA and MA→TGA in combination for 6 h due to the increased amounts of partial hydrolyzed AP molecules.

The CLD profiles of debranched samples examined by GPC (Fig. 3B) discriminated three main components: short amylopectin (DP 6-36), long amylopectin (DP 37-100) and amylose chains (DP > 100) (Zhong et al., 2020). The main structural changes we observed was the degradation of amylose chains caused by TGA alone, MA alone, and MA→TGA in combination. TGA alone hydrolyzed the amylose chains possibly due to the existence of some amylose chains on the surface of granules (Glaring, Koch, & Blennow, 2006). The figure also showed that MA and

TGA not only hydrolyzed amylopectin molecules but also hydrolyzed the amylose molecules. The slight increase in molecular size between the 6 h TGA and 20 h TGA samples, was confirmed specifically in the AP2 and AM regions.

3.3. High-performance anion exchange chromatography-pulsed amperometric detection (HPAEC-PAD)

How close to branch points an α-1,4 glucanase will cleave on the side chains of starch defines what the ultimate limit dextrin product structure will be. The debranched enzyme-modified starches were therefore subject to HPAEC-PAD to obtain a higher resolution of the short amylopectin chains. The resulting CLDs obtained from the native maize starches and their derivatives MA, TGA and MA→TGA starches (Fig. 3C and D) showed significant effects of MA and MA→TGA on AP CLDs. The CLDs determined from the buffer incubated starch and the TGA incubated starches showed a similar distribution to the native starch. The addition of MA shifts the distribution towards the shorter chains. A relative increase was observed for branches from DP 2-9, especially from DP 2-4, while the amylopectin chains ranging DP 10-28 were greatly reduced (Fig. 3D). With the addition of TGA, the DP 2 peak was further amplified to cover >6 % for the measured chromatogram.

3.4. Wide-angle X-ray scattering (WAXS)

WAXS patterns of the samples (Fig. 4A) show that the crystalline polymorph was not affected by the enzymatic modification. All starches
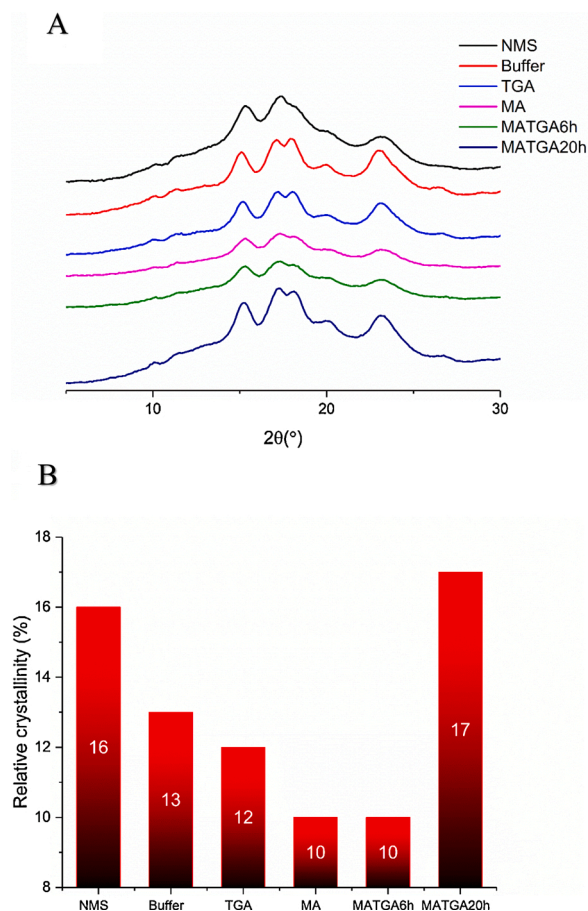
Fig. 4. A) XRD patterns; B) the relative crystallinity of starches.

Fig. 5. One-dimensional ^{1}H NMR spectra of enzyme-treated starch samples.

Table 2
The parameters from proton nuclear magnetic resonance spectroscopy (^{1}H NMR).

Samples	α-1,6 : α-1,4 ratio (%)
NMS	3.07
Buffer	3.68
TGA	5.81
MA	7.43
MATGA6 h	7.28
MATGA20 h	8.07

displayed the A-type allomorph with strong diffraction peaks at 2θ around 15° and 23°, and an unresolved doublet at 2θ 17° and 18° (Cheetham & Tao, 1998). However, the crystallinity was altered by the modification (Fig. 4B). The buffer incubated starch showed a lower crystallinity than native starch, showing the degradation of normal maize starch from the crystalline structure level, which is consistent with the degradation monitored from the molecular structure level. This is in contrast to our previous study of rice starch showing that incubation of the starch in buffer significantly increased the crystallinity (Keeratiburana, Hansen, Soontaranon, Blennow et al., 2020). This discrepancy cannot be explained; both starch types have similar amylose contents, however, the granular size, which is considerably smaller for rice starch, might be decisive for this differential effect. TGA only modified starch showed a similar crystallinity to that of buffer only incubated sample, implying TGA alone cannot modify the crystalline structure of NMS. On the other hand, MA lowered the crystallinity of starch efficiently through its α-(1→4)-glycosidic hydrolyzing activity (Ao et al., 2007). On the contrary, for rice starch, MA increased the crystallinity, which was explained as an effect of the preferable hydrolytic attack of the amorphous regions of rice starch (Keeratiburana, Hansen, Soontaranon, Blennow et al., 2020). Our data on maize starch showed that MA possibly preferentially attacked the crystalline regions of the starch granules suggesting a higher enzymatic susceptibility of maize granules compared to rice granules with similar amylose contents. Interestingly, 6 h TGA post-treatment had no further effect on crystallinity, while 20 h TGA post-treatment dramatically increased the crystallinity, which is further discussed below
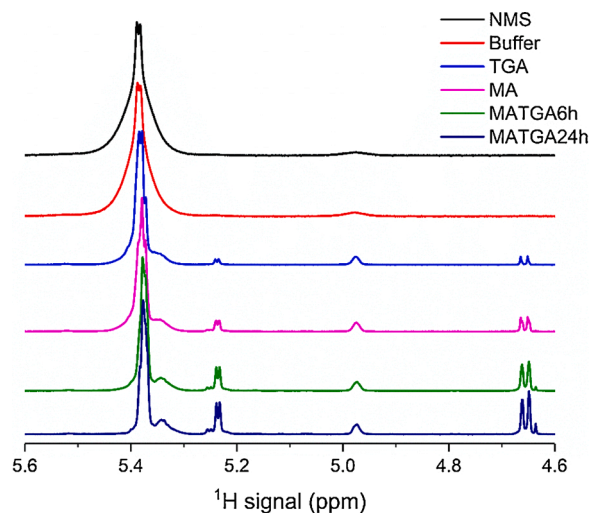
3.5. H NMR spectroscopy

The ^{1}H NMR spectra (Fig. 5) displayed four peaks of starches in the region of 4.6 to 5.6 ppm. The peaks in 5.39 and 4.99 ppm correspond to the anomeric protons of α-1,4 and α-1,6 linkages, respectively (Bai, Shi, Herrera, & Prakash, 2011). The effects of MA alone, TGA alone, and MA→TGA gradually increased the relative ratio of α-1,6 to α-1,4 linkages (Table 2), showing that MA pre-treatment was mainly responsible for the increase of α-1,6 linkages supposedly by trimming down external chains by its exo-activity. The signals at 5.23 and 4.65 ppm originate from the α- and β-anomeric reducing end protons, respectively (Bai et al., 2011), both of which were increased by the enzyme treatments suggesting excessive hydrolysis. However, these signals are much too intense to account for possible reducing ends and there are additional signals at higher ppm, close to the α-anomeric region and at lower ppm close to the β-anomeric region, indicating superimposed signals not origination from anomeric protons i.e. from transfer reactions or specific strain on the glucose ring.

3.6. Rheological behavior

Pasting behavior as analyzed by RVA (Fig. 6A) showed slight decreases of pasting viscosities for the buffer control and the TGA treated starch (Fig. 6A). However, notable decreases in pasting viscosities were found for the MA treated starch and for the MA→TGA starches. The peak viscosity is mainly affected by the swelling and integrity of swelled starch granules (Crosbie, 1991), and thus the decrease in peak viscosity observed was dependent on the disruption degree of granules due to the enzymatic hydrolysis. The swelling power data (not shown) was consistent with the changes of peak viscosity. It worth mentioning that MA and MA→TGA 20 h treatments significantly decreased the setback viscosity of the starch (Fig. 6B), indicating MA and MA→TGA treatments reduced short-term retrogradation (recrystallization) of the starch upon
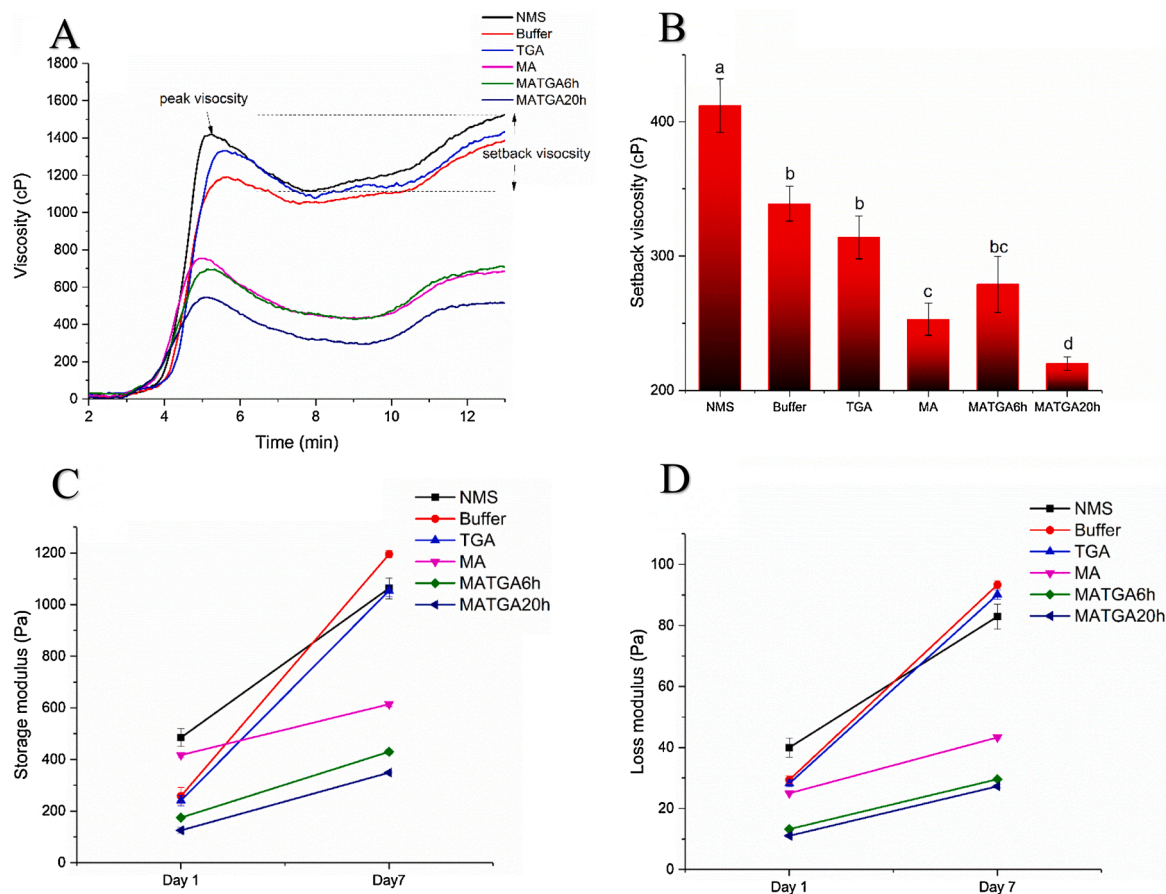
Fig. 6. a) RVA profiles; b) setback viscosity; c) storage modules, d) loss modulus of samples.

cooling. The increase in branch points in the MA and MA→TGA samples reduced starch retrogradation to some degree which is following other studies (Guo, Tao et al., 2019).

The rheological data showed notable variations of the storage modulus (G′) and the loss modulus (G″) for starch pastes stores for 1 day and 7 days (Fig. 6 C and D). The G′, indicating the strength of gels, and the G″, indicating the dissipated energy (viscosity) of a paste showed that all samples had G′ that was higher than G″, indicating typical gel-behavior of samples. MA, MA→TGA 6 h, and MA→TGA 20 h showed the lower difference in these moduli than the NMS, Buffer control and TGA samples, indicating higher stability, i.e. lower molecular rearrangement, in these samples. This effect can be attributed to their higher content of short amylopectin chains and lower molecular weights (Fig. 3C and D) as also demonstrated previously (Guo, Tao et al., 2019). In comparison with the MA treated sample, TGA post-treatment had no effect on the relative rheological changes of G′ and G″ from day 1 to day 7, but significantly lowered the values of both G′ and G″. Hence, the MA→TGA samples formed weaker gels and lower viscous systems than MA. The molecular structure data showed that the main consistent changes in the molecular structure were the reduction in amylopectin chains with DP 10-28, which were reduced in the order of NMS, Buffer, TGA, MA and MA→TGA samples. Therefore, we suggest the content of amylopectin chains with DP 10-28 was possibly the main factor affecting the gel formation and rearrangement.

3.7. The underlying mechanism of sequential MA and TGA modification on granular starch

We found that MA attacked maize starch granules by producing pores, thereby hydrolyzing the amylopectin and amylose molecules, especially side chains of amylopectin with DP 10-28, and producing more short amylopectin chains with DP < 10 (Fig. 3D). WAXS analysis showed that MA treatment decreased the relative crystallinity (Fig. 4B), suggesting that the hydrolytic effect of MA was primarily on the crystalline regions of the starch granules. In contrast, for rice starch, MA mainly attacks the amorphous regions a evidenced from increased crystallinity of this starch (Keeratiburana, Hansen, Soontaranon, Blennow et al., 2020). Possibly this effect is due to differentially assembled glucan material in the granules. Rice starch granules were found to be more enzymatic resistant than maize starch granules to MA as evidenced by the higher MA dosage required for the maize starch to get an effect. Such different molecular packing can provide different hydrolytic action for MA in relation to crystalline and amorphous material. As expected, MA increased the relative branching degree of starch (Table 2), thereby decreasing the retrogradation rate of maize starch as monitored by RVA (Fig. 6B) and rheological analysis (Fig. 6C).

In comparison to MA, TGA virtually lacked the ability to modify maize starch alone as confirmed by the unchanged molecular structure and crystallinity and that TGA failed to enter the inside of granules and stayed on the surface of granules (Fig. 2B). However, very minor channels were seen and TGA still had some transglycosylation effect which was proved by the increasing degree of branching (Table 2). A similar phenomenon was found in potato starch (Guo, Deng, Lu, Zou, & Cui, 2019). On the other hand, based on the MA pre-treatment, TGA got access and started to modify the interior of granules (Fig. 2D). In the first 6 h, TGA mainly showed a hydrolytic effect, since larger pores were found in the granule surface (Fig. 1E) and amylopectin (Fig. 3A) and amylose (Fig. 3B) molecules were further hydrolyzed. The NMR data confirmed that the branching degree remained unchanged and that there were possible yet un-identified bonds formed (Table 2, Fig. 5). The unchanged crystallinity (Fig. 4B) and significantly decreased yield from MA to MA→TGA 6 h (Table 1) suggest that the hydrolysis of TGA on
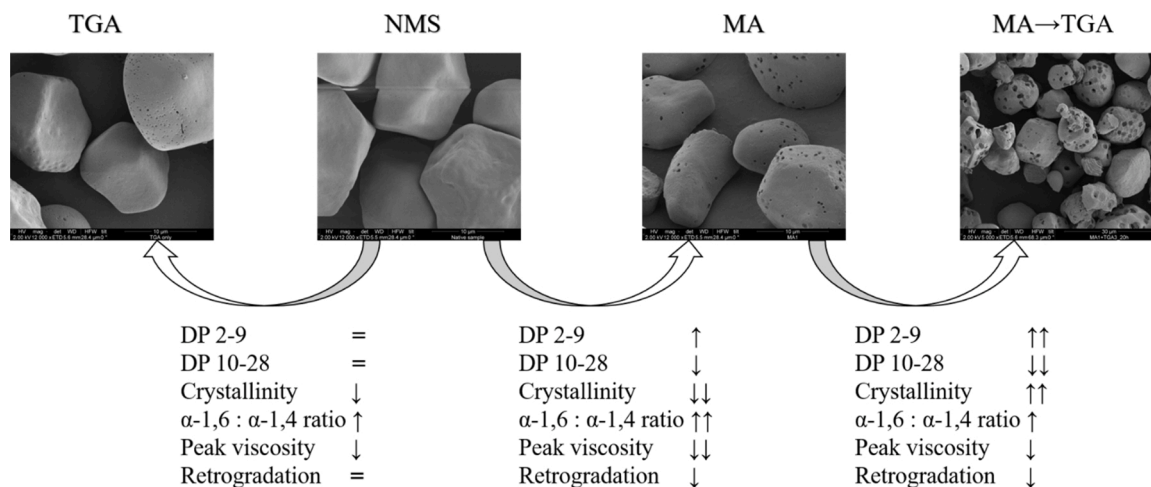
Fig. 7. A model describing the effects of MA and TGA on granular maize starch.

granules attacked both the amorphous and the crystalline regions similarly. In the next 14 h, we did not see a further decrease in amylopectin molecule size (Fig. 3A) but the degree of branching was increased (Table 2). Hence, TGA increasingly showed transglycosylation, and produced large amounts of amylopectin short chains with DP < 10 supposedly by transfer from chains with DP 10-28 (Fig. 3D). As an effect, retrogradation of starch was further decreased by TGA as observed by RVA and rheology (Fig. 6 B,C). The dramatic increase in crystallinity found for the long term TGA treatment may have different possible reasons. Either TGA excessively hydrolyzed the amorphous regions of the starch granules, thereby increasing the relative crystallinity or TGA improved the crystal ordering through its transglycosylation and hydrolytic reactions leading to recrystallization (Ao et al., 2007). It is worth mentioning that the NMR signals found at 5.23 and 4.65 ppm are most often referred to anomeric sites (Bai et al., 2011), i.e. in our case originating for hydrolytic cleavage. However, they are far too strong to account only from anomeric protons and the regions around these signals were more complex with additional signals. Transfer to the 2- and 3 carbons by TGA can occur (Sorndech, Tongta, & Blennow, 2018) and strained glucosidic conformations such as the H1 chemical shift at 5.26 in the cyclic maltosyl-(1→6)-maltose produced by *Arthrobacter globiformis* (Mukai et al., 2005) indicate that such protons can contribute to the increase of the signals in the anomeric regions. These structures possibly originate from close branching structures but remain to be identified. An underlying model was adopted to describe the effects of MA and TGA on granular starch (Fig. 7).

4. Conclusion

In this study, we explored the sequential enzyme modifications of native maize starch granules using maltogenic α-amylases (MA) and transglucosidase (TGA). MA increased the enzyme susceptibility of granules for TGA post modification, by providing narrow internal pores in granules. First, TGA mainly hydrolyzed the starch granules, but it produced new α-1, 6 linkages. TGA following MA-treatment produced a large number of amylopectin chains with DP < 10 and decreased crystallinity, however, prolonged incubation increased the granular crystallinity. In addition to branching, hydrolysis occurred and yet unidentified bonds or conformations were formed. Enzyme treatment decreased retrogradation, and the storage-dependent increase of both storage- and loss moduli.

Funding

CRediT authorship contribution statement

Yuyue Zhong: Conceptualization, Investigation, Methodology, Software, Writing - original draft, Writing - review & editing. **Thewika Keeratiburana:** Investigation, Data curation. **Andreas Blennow:** Resources, Conceptualization, Funding acquisition, Supervision. **Aleksander Riise Hansen:** Resources, Conceptualization, Funding acquisition, Supervision.

References

Ao, Z., Simsek, S., Zhang, G., Venkatachalam, M., Reuhs, B. L., & Hamaker, B. R. (2007). Starch with a slow digestion property produced by altering its chain length, branch density, and crystalline structure. *Journal of Agricultural and Food Chemistry, 55*(11), 4540–4547.

Bai, Y., Shi, Y.-C., Herrera, A., & Prakash, O. (2011). Study of octenyl succinic anhydride-modified waxy maize starch by nuclear magnetic resonance spectroscopy. *Carbohydrate Polymers, 83*(2), 407–413.

Benavent-Gil, Y., & Rosell, C. M. (2017). Comparison of porous starches obtained from different enzyme types and levels. *Carbohydrate Polymers, 157*, 533–540.

Blazek, J., & Gilbert, E. P. (2010). Effect of enzymatic hydrolysis on native starch granule structure. *Biomacromolecules, 11*(12), 3275–3289.

Blennow, A., Bay-Smidt, A. M., Wischmann, B., Olsen, C. E., & Møller, B. L. (1998). The degree of starch phosphorylation is related to the chain length distribution of the neutral and the phosphorylated chains of amylopectin. *Carbohydrate Research, 307*(1), 45–54.

Blennow, A., Hansen, M., Schulz, A., Jørgensen, K., Donald, A. M., & Sanderson, J. (2003). The molecular deposition of transgenically modified starch in the starch granule as imaged by functional microscopy. *Journal of Structural Biology, 143*(3), 229–241.

Brückner, S. (2000). Estimation of the background in powder diffraction patterns through a robust smoothing procedure. *Journal of Applied Crystallography, 33*(3), 977–979.

Cheetham, N. W. H., & Tao, L. (1998). Variation in crystalline type with amylose content in maize starch granules: An X-ray powder diffraction study. *Carbohydrate Polymers, 36*(4), 277–284.

Christophersen, C., Otzen, D. E., Noman, B. E., Christensen, S., & Schäfer, T. (1998). Enzymatic characterisation of novamyl®, a thermostable α-amylase. *Starch - Stärke, 50*(1), 39–45.

Crosbie, G. B. (1991). The relationship between starch swelling properties, paste viscosity and boiled noodle quality in wheat flours. *Journal of Cereal Science, 13*(2), 145–150.

Glaring, M. A., Koch, C. B., & Blennow, A. (2006). Genotype-specific spatial distribution of starch molecules in the starch granule: A combined CLSM and SEM approach. *Biomacromolecules, 7*(8), 2310–2320.

Goldstein, A., Annor, G., Vamadevan, V., Tetlow, I., Kirkensgaard, J. J., Mortensen, K., … Bertoft, E. (2017). Influence of diurnal photosynthetic activity on the morphology, structure, and thermal properties of normal and waxy barley starch. *International Journal of Biological Macromolecules, 98*, 188–200.

Guo, L., Deng, Y., Lu, L., Zou, F., & Cui, B. (2019). Synergistic effects of branching enzyme and transglucosidase on the modification of potato starch granules. *International Journal of Biological Macromolecules, 130*, 499–507.

Guo, L., Li, H., Lu, L., Zou, F. X., Tao, H. T., & Cui, B. (2019). The role of sequential enzyme treatments on structural and physicochemical properties of cassava starch granules. *Starch-Starke, 71*(7–8).

Guo, L., Tao, H., Cui, B., & Janaswamy, S. (2019). The effects of sequential enzyme modifications on structural and physicochemical properties of sweet potato starch granules. *Food Chemistry, 277*, 504–514.

Huber, K., & BeMiller, J. (2000). Channels of maize and sorghum starch granules. *Carbohydrate Polymers, 41*(3), 269–276.

Keeratiburana, T., Hansen, A. R., Soontaranon, S., Blennow, A., & Tongta, S. (2020). Porous high amylose rice starch modified by amyloglucosidase and maltogenic α-amylase. *Carbohydrate Polymers, 230*, Article 115611.

Keeratiburana, T., Hansen, A. R., Soontaranon, S., Tongta, S., & Blennow, A. (2020). Porous rice starch produced by combined ultrasound-assisted ice recrystallization and enzymatic hydrolysis. *International Journal of Biological Macromolecules, 145*, 100–107.

Li, Y., Li, C., Gu, Z., Hong, Y., Cheng, L., & Li, Z. (2017). Effect of modification with 1, 4-α-glucan branching enzyme on the rheological properties of cassava starch. *International Journal of Biological Macromolecules, 103*, 630–639.

Mukai, K., Watanabe, H., Oku, K., Nishimoto, T., Kubota, M., Chaen, H., & Kurimoto, M. (2005). An enzymatically produced novel cyclic tetrasaccharide, cyclo-{→ 6)-α-D-Glcp-(1→ 4)-α-D-Glcp-(1→ 6)-α-D-Glcp-(1→ 4)-α-D-Glcp-(1→}(cyclic maltosyl-(1→ 6)-maltose), from starch. *Carbohydrate Research, 340*(8), 1469–1474.

Naguleswaran, S., Li, J., Vasanthan, T., & Bressler, D. (2011). Distribution of granule channels, protein, and phospholipid in triticale and corn starches as revealed by confocal laser scanning microscopy. *Cereal Chemistry, 88*(1), 87–94.

Ota, M., Okamoto, T., & Wakabayashi, H. (2009). Action of transglucosidase from Aspergillus niger on maltoheptaose and [U–13C] maltose. *Carbohydrate Research, 344*(4), 460–465.

Ota, M., Okamoto, T., Hoshino, W., & Wakabayashi, H. (2009). Action of α-D-glucosidase from Aspergillus niger towards dextrin and starch. *Carbohydrate Polymers, 78*(2), 287–291.

Rydahl, M. G., Hansen, A. R., Kračun, S. K., & Mravec, J. (2018). Report on the current inventory of the toolbox for plant cell wall analysis: Proteinaceous and small molecular probes. *Frontiers in Plant Science, 9*, 581.

Satoru Ishihara, K. (2017). In A. E. INC (Ed.), *Modified alpha-glucosidase and applications of same* (Vol. 9650619). Japan: AMANO Enzyme Inc.. https://patents.google.com/patent/US9650619/und

Shi, M., Zhang, Z., Yu, S., Wang, K., Gilbert, R. G., & Gao, Q. (2014). Pea starch (Pisum sativum L.) with slow digestion property produced using β-amylase and transglucosidase. *Food Chemistry, 164*, 317–323.

Song, Z., Zhong, Y., Tian, W., Zhang, C., Hansen, A. R., Blennow, A., … Guo, D. (2019). Structural and functional characterizations of α-amylase-treated porous popcorn starch. *Food Hydrocolloids*, Article 105606.

Sorndech, W., Tongta, S., & Blennow, A. (2018). Slowly digestible-and non-digestible α-glucans: An enzymatic approach to starch modification and nutritional effects. *Starch-Stärke, 70*(9–10), Article 1700145.

Szymońska, J., & Wodnicka, K. (2005). Effect of multiple freezing and thawing on the surface and functional properties of granular potato starch. *Food Hydrocolloids, 19*(4), 753–760.

Wang, S., & Copeland, L. (2012). Phase transitions of pea starch over a wide range of water content. *Journal of Agricultural and Food Chemistry, 60*(25), 6439–6446.

Wickramasinghe, H. A. M., Blennow, A., & Noda, T. (2009). Physico-chemical and degradative properties of in-planta re-structured potato starch. *Carbohydrate Polymers, 77*(1), 118–124.

Zhang, C., Han, J.-A., & Lim, S.-T. (2018). Characteristics of some physically modified starches using mild heating and freeze-thawing. *Food Hydrocolloids, 77*, 894–901.

Zhong, Y., Liu, L., Qu, J., Blennow, A., Hansen, A. R., Wu, Y., … Liu, X. (2020). Amylose content and specific fine structures affect lamellar structure and digestibility of maize starches. *Food Hydrocolloids*, Article 105994.